

Influence of temperature on the reactivity of phosphorus acid esters in reverse micellar systems based on sodium bis(2-ethylhexyl)sulfosuccinate

L. Ya. Zakharova,^{a*} A. R. Ibragimova,^a F. G. Valeeva,^a V. M. Zakharov,^a
L. A. Kudryavtseva,^a A. I. Konovalov,^a N. L. Zakharchenko,^a and Yu. F. Zuev^b

^aA. E. Arbuzov Institute of Organic and Physical Chemistry,
Kazan Research Center of the Russian Academy of Sciences,
8 ul. Akad. Arbuzova, 420088 Kazan, Russian Federation.
Fax: +7 (843 2) 73 2253. E-mail: lucia@iopc.knc.ru

^bKazan Institute of Biochemistry and Biophysics,
Kazan Research Center of the Russian Academy of Sciences,
p.o. 30, 420111 Kazan, Russian Federation

A change in the reactivity of ethyl *p*-nitrophenyl chloromethylphosphonate in the sodium bis(2-ethylhexyl)sulfosuccinate–*n*-nonane–water system around the percolation threshold was found. Study of location sites of the reactants by NMR self-diffusion and optical spectroscopy and modeling of the kinetic data in terms of the pseudophase approach demonstrated that below the percolation threshold, the reaction occurs in the surface layer. The observed rate constant for substrate hydrolysis in a microemulsion below the percolation threshold is described by the Arrhenius equation, like that in aqueous solutions. Above the percolation threshold, the slope of the Arrhenius plot sharply changes, which is apparently due to a change in the reactant location pattern and, hence, the microscopic properties of the medium in the region of their solubilization.

Key words: reverse micelles, microemulsions, kinetics, hydrolysis, phosphorus acid esters, percolation, pseudophase model.

The reverse micellar systems are thermodynamically stable dispersions of nano-sized water drops in an organic liquid (oil) stabilized by a surfactant monolayer. A frequently used surfactant is sodium bis(2-ethylhexyl)sulfosuccinate (Aerosol OT, AOT). The branched molecules of this surfactant allow the formation of reverse micelles (region L₂ in the phase diagram of microemulsion) without the addition of other surfactants over a broad range of temperatures and compositions.¹ The reverse micellar systems offer broad possibilities for the deliberate control of the rates and mechanisms of chemical reactions.²

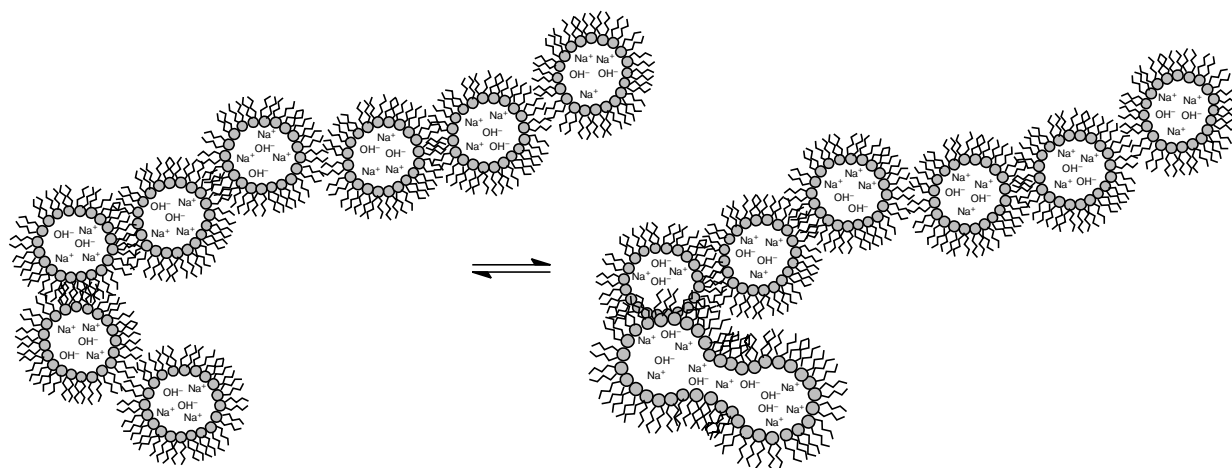
The continuous phase in these systems is formed by nonpolar organic liquids; hence, its conductivity is relatively low and determined by the exchange of ions formed upon dissociation of the head groups of ionic surfactants between the reverse micelles during their thermal motion and random collisions. Under certain conditions (for example, on temperature rise), the conductivity of such systems sharply increases by four to five orders of magnitude.^{3,4} This phenomenon, which has been called electric percolation, is due⁵ to clusterization of reverse micelles

and charge migration within extended clusters (Scheme 1). The conditions for micelle adhesion, short-term coalescence, and return to the initial state are determined, first of all, by the properties of the hydrophobic surface of reverse micelles. A necessary condition for the temporal coalescence of particles is the mutual penetration of the hydrocarbon radicals of the interacting micelles, which depends on the structural organization of the surfactant surface layer.⁶

Clusterization of AOT-based reverse micelles is observed over a broad range of concentrations of the disperse phase and reflects the changes taking place in the structure of the micelle hydrophobic shells on temperature rise. This induces a change in the physicochemical parameters of the compound microenvironment (viscosity, polarity, *etc.*), which can influence the kinetics of chemical reactions in these media.

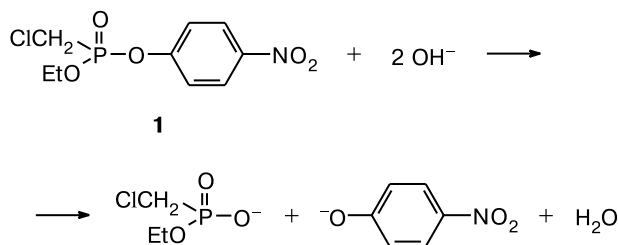
As we have shown previously,⁷ the structural rearrangement of reverse micelles affects the reactivity of phosphorus acid esters. To elucidate the causes and the mechanism of this relationship, we continued the studies of the catalytic effect of an AOT-based reverse micellar system.

Scheme 1



This work is devoted to the kinetics of alkaline hydrolysis of ethyl *p*-nitrophenyl chloromethylphosphonate (**1**) in the AOT—*n*-nonane—water system (Scheme 2) at temperatures below and above the spontaneous clusterization threshold. In addition, location sites of the substrate in the reverse micelles were determined by the NMR self-diffusion technique.

Scheme 2



Experimental

Compound **1** was prepared by a known procedure;⁸ commercial AOT (Sigma) was used as received. The reverse micellar systems were prepared by adding a calculated amount of water to a solution of AOT in *n*-nonane of a specified concentration followed by vigorous shaking of the mixture until a transparent solution formed. The molar ratios of the components, namely, $W = [\text{H}_2\text{O}]/[\text{AOT}]$, characterizing the size of the water cores of the micelles, and $Z = [n\text{-nonane}]/[\text{AOT}]$, characterizing the micelle concentration, were varied in the 9.8–37.6 and 5–22 ranges, respectively, corresponding to the region L_2 in the system phase diagram.⁹

The conductivity was measured by an OK 102/1 conductometer (Radelkis, Hungary) at frequencies of 80 Hz and 3 kHz in a parallel-sided cell maintained in a thermostat. The temperature was controlled to an accuracy of $\pm 0.2^\circ\text{C}$.

The self-diffusion coefficients (D) were measured by Fourier Transform ^1H NMR spectroscopy with a pulse magnetic field gradient¹⁰ using a modified Tesla BS 587 A NMR spectrometer operating at a frequency of 80 MHz (for ^1H) and equipped with a gradient block designed for producing a magnetic field gradient of up to 0.5 T m^{-1} . The self-diffusion coefficients were determined from the individual proton signals of system components using a standard two-pulse Hahn sequence. The error of determination of the coefficients did not exceed 5%.

The kinetics of hydrolysis was studied by spectrophotometry on a Specord M-400 instrument based on the variation of absorption of the leaving-group anion under the pseudo-first order conditions. The observed rate constants (k_{obs}) were found from the dependence

$$\ln(A_\infty - A) = -k_{\text{obs}}t + \text{const},$$

where A and A_∞ are the solution absorbances at time instant t and after completion of the reaction, respectively. They were found using the weighed least-squares method taking into account the arithmetic mean values of the three measurements differing by at most 5%.

The kinetic data were analyzed using a pseudophase model according to which the reactants are distributed among the phases and the reaction proceeds in one or several pseudophases. For reactions that proceed in the surface layer, while one reactant (substrate) is distributed between the oil phase and the surfactant monolayer and the other reactant (hydroxide ion) is distributed between the surface layer and water, the equation for the observed rate constant has the form¹¹

$$k_{\text{obs}} = (k_i K_S K_{\text{OH}} [\text{OH}]_{\text{tot}}) / \{(K_S + Z)(K_{\text{OH}} + W)[\text{AOT}]\}, \quad (1)$$

where k_i/s^{-1} is the rate constant for the bimolecular reaction provided that the nucleophile concentration is expressed as the $[\text{OH}]/[\text{AOT}]$ molar ratio; K_S is the partition constant of the substrate (S) between the oil phase and the surfactant; K_{OH} is the partition constant of the hydroxide ion between the aqueous phase and the surfactant; $[\text{OH}]_{\text{tot}}/\text{mol L}^{-1}$ is the total concentration of the OH^- ions. The constant k_i is related to the tradi-

tional pseudo-first (k_i'/s^{-1}) and second ($k_{2,i}/L \text{ mol}^{-1} s^{-1}$) order rate constants by the following relations:

$$k_i' = k_i([OH]/[AOT]),$$

$$k_{2,i} = k_i V,$$

where V is the molar volume of the surfactant. The constants K_S and K_{OH} are given by

$$K_S = ([S]_i[n-C_9H_{20}])/([S]_o[AOT]),$$

$$K_{OH} = ([OH]_i[H_2O])/([OH]_w[AOT]).$$

Here, the molar concentrations of the substrate (S), *n*-nonane, and surfactant are given in brackets and the subscripts i, o, and w refer to the surface layer, oil, and water pseudophases, respectively. The main assumptions and approximations used in the pseudophase model have been considered previously.¹² The linearized form of the equation (1)

$$1/(k_{obs}[AOT]) = (K_{OH} + W)/(k_i K_{OH}[OH]) + \{(K_{OH} + W)/(k_i K_S K_{OH}[OH])\}Z \quad (2)$$

allows one to calculate the K_S , K_{OH} , k_i , and $k_{2,i}$. It can be seen from Eq. (2) that the binding constant of the substrate K_S can be determined graphically using the plot $1/(k_{obs}[AOT])$ — Z from the ratio of the y-intercept to the slope of the plot. This model implies that the K_S value does not change upon the variation of W .

Results and Discussion

According to the conductometric data shown in Fig. 1, the percolation threshold temperature (T_p) in the AOT—*n*-nonane—water system is 26–38 °C depending on the parameter W . Previously,⁷ we discovered some increase in the percolation threshold temperature with an increase in the alkali concentration; however, for $[NaOH] = 0.01 \text{ mol L}^{-1}$, which was maintained in the experiment, this effect is insignificant. The results of conductivity measurements were used to choose conditions for the kinetic measurements before and after the micelle clusterization threshold, which was defined as the temperature of the sign change of the second derivative of the conductivity with respect to temperature.

The self-diffusion coefficients D of the system components found by NMR¹⁰ spectroscopy are presented in Fig. 2. Owing to the specific features of AOT-stabilized reverse micellar systems, it was possible to use micelle clusterization for determining the substrate location sites in the reverse micelles. Although compound **1** is rather hydrophobic, its structure implies accumulation not only in the oil pseudophase but also in other microregions of the system. It is reasonable to suggest that if compound **1** is completely dissolved in *n*-nonane, the temperature dependence of its self-diffusion coefficient plotted in the Arrhenius coordinates would be parallel to the dependence of the self-diffusion coefficient of *n*-nonane. The absolute D values for phosphonate **1** dissolved in the oil

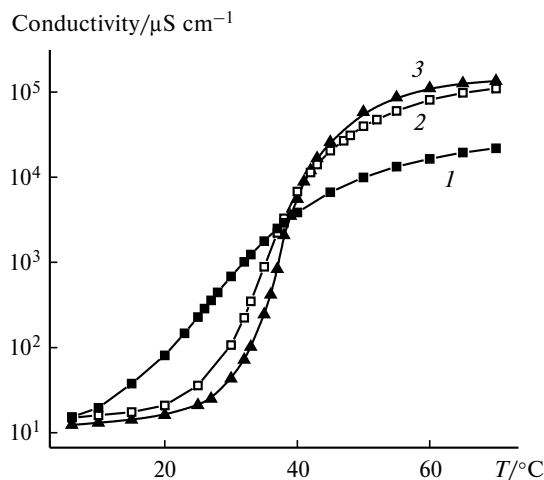


Fig. 1. Conductivity of the AOT—*n*-nonane—water system vs. temperature at $W = 9.8$ (1), 15.1 (2), and 20.0 (3) ($C_{AOT} = 0.4 \text{ mol L}^{-1}$).

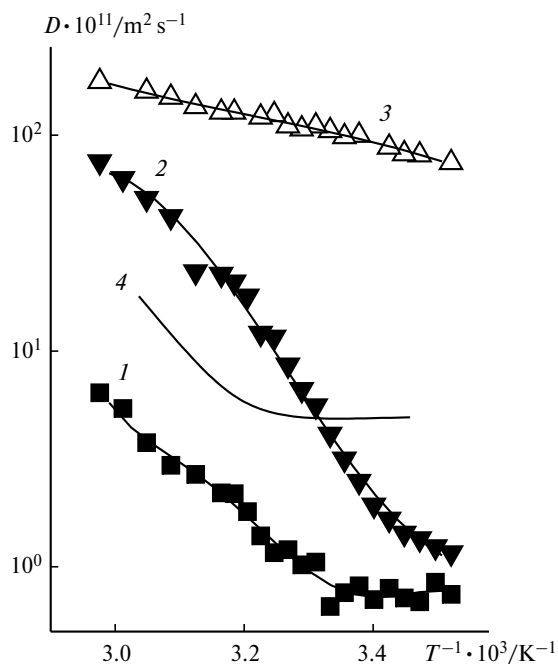


Fig. 2. Temperature dependences of the self-diffusion coefficients (D) of components of the AOT—*n*-nonane—water system: AOT (1), water (2), *n*-nonane (3), *p*-nitrophenyl ethyl chloromethylphosphonate (4) ($W = 20.0$, $C_{AOT} = 0.4 \text{ mol L}^{-1}$).

phase should not differ much from the D value for *n*-nonane as the sizes of their molecules are similar. In reality, the coefficient D found experimentally for compound **1** in this system is intermediate between the values for AOT (micelle diffusion) and *n*-nonane. The exponential pattern of the diffusion decay of the resonance signal from the protons of compound **1** suggests that this compound is distributed between the disperse phase and the dispersion medium. These two states undergo fast (on

the NMR time scale) exchange. Using the two-state model,^{13,14} we found that 52% of the substrate is dissolved in the dispersion medium (*n*-nonane), while the rest is located in the reverse micelles. The site of location of compound **1** in the reverse micelles is determined by analyzing the temperature dependence of the self-diffusion coefficient. Provided that phosphonate **1** is located in the aqueous cores of the micelles, the temperature variations of its diffusion are expected to reproduce the temperature variations of water diffusion. It follows from the data presented in Fig. 2 that the temperature dependence of the self-diffusion coefficient of compound **1** reflects the temperature variation of the self-diffusion coefficient of AOT, which is due to the substrate accumulation in the surfactant monolayer. Thus, phosphonate **1** is distributed between the *n*-nonane bulk and the micelles in which it is located in the surface layer formed by AOT molecules.

We studied the kinetics of hydrolysis of phosphonate **1** at different temperatures covering a range below and above the percolation threshold. The plots $\log k_{\text{obs}} - 1/T$ for various W ($C_{\text{AOT}} = 0.4 \text{ mol L}^{-1}$, $C_{\text{NaOH}} = 0.01 \text{ mol L}^{-1}$) are presented in Fig. 3. Unlike aqueous solutions, in reverse micellar systems, the usual Arrhenius dependence holds only up to a certain, critical temperature (T_{cr}). Comparison of the data presented in Figs 1 and 3 shows that the T_{cr} and T_{p} values are almost equal for equal W values (Table 1). We assume that the change in the slope of the Arrhenius plot is related to those temperature-induced structural changes in reverse micelles that induce clusterization. Evidently, this may be accompanied by changes in some characteristics of the micellar microenvironment of the reactants (micropolarity, surface potential, etc.), which affect the reactivity.

The temperature dependence of the rate constant for chemical reactions in solutions is known¹⁵ to be described by the Arrhenius equation. Unlike molecular solutions, micellar media are microheterogeneous. The kinetics of these systems is often described using the pseudophase approach according to which the reaction may occur in three microregions: in the oil and aqueous pseudophases and in the surface layer. In this case, the equation for the observed rate constant has three constituents.¹⁶ In this

Table 1. Values of T_{p} and T_{cr} and Arrhenius equation parameters below the percolation threshold (activation energy (E_{a}) and pre-exponential factor ($\log A$)) for alkaline hydrolysis of phosphonate **1** in the AOT–*n*-nonane–water reverse micellar system

W	T_{p}	T_{cr}	E_{a}	$\log A$
	$^{\circ}\text{C}$		kJ mol^{-1}	
9.8	26	25	31.5	3.7
15.1	35	32	31.2	3.5
20.0	37	36	26.7	2.7

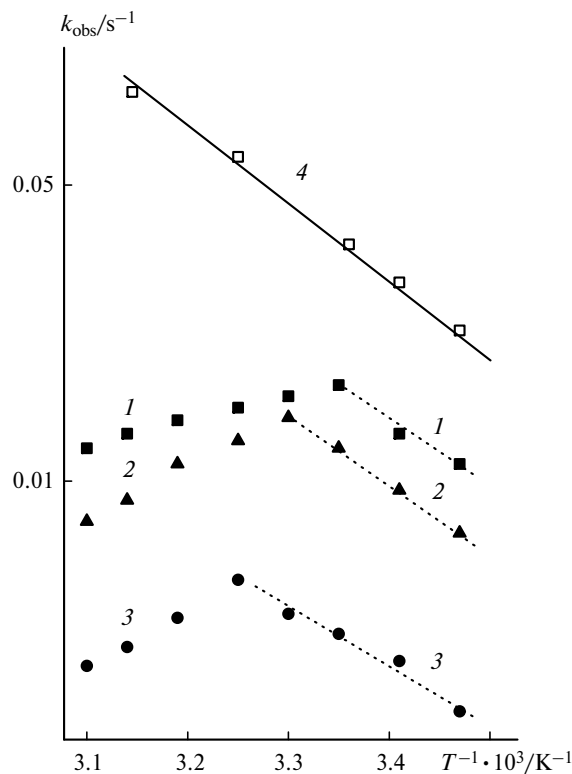


Fig. 3. Arrhenius dependence of the observed rate constant for the alkaline hydrolysis of phosphonate **1** (k_{obs}) in the AOT–*n*-nonane–water reverse micellar system at $W = 9.8$ (1), 15.1 (2), and 20.0 (3) and in water (4) ($C_{\text{NaOH}} = 0.01 \text{ mol L}^{-1}$, $C_{\text{AOT}} = 0.4 \text{ mol L}^{-1}$).

study, we consider a simpler situation where the reaction zone is assumed to be limited to the surface layer and the observed rate constant is described by Eq. (1). According to the known data,^{11,12} the rate of a chemical reaction should not depend on the micelle formation dynamics or reactant exchange between the pseudophases. The fulfillment of the Arrhenius equation then depends on the degree to which the binding constants are temperature-dependent. In micellar systems in the absence of phase transitions, the binding constants of the reactants depend on the temperature; however, the contribution of these changes to the observed rate constant can be neglected compared with the case of exponential variation of the rate constant, especially in a narrow temperature range. When the $\log k_{\text{obs}} - 1/T$ plot is linear, analysis of the kinetic data in micellar solutions allows one to calculate the activation energy.

The properties of the microdrops in which the chemical reaction occurs are also subject to the influence of the temperature. For the system under study, this influence is most pronounced around the temperature percolation threshold. In view of the complex structure of the microemulsion and the presence of the polarity gradient in the surface layer, not only a quantitative change in the parti-

tion coefficients of the reactants is possible under temperature perturbation conditions, but also qualitative changes, resulting in the migration of the reaction zone. In this case, additional influence of the temperature on the observed rate constant is expected, due to the change of the microscopic properties in the reaction zone. In a simplified form, this effect can be compared with change of the solvent, and is not necessarily described by the Arrhenius equation.

Therefore, the effect of temperature on the reaction kinetics in reverse micellar systems can be separated into two components. One is related to the usual thermal activation of chemical processes, while the other is due to the change in the reactant location sites and partition coefficients in the system due to modification of the properties of aggregates. The usual course of the Arrhenius dependence (see Fig. 3) at $T < T_{cr}$ indicates that the former component makes a predominant contribution. In this case, the slope of the $\log k_{obs} - 1/T$ plot is described by the activation energy (E_a) of the alkaline hydrolysis of substrate **1**. Above the critical temperature, the competitive trend predominates, the pattern of the dependence being determined by the change in the local properties of the reactant microenvironment with temperature. In the region $T > T_{cr}$, k_{obs} decreases following an increase in T . Although the linearity in the $\log k_{obs} - 1/T$ coordinates holds, it is hardly reasonable to speak of the fulfillment of the Arrhenius equation. With this data interpretation, which is shown in Fig. 3, it becomes clear that T_{cr} coincides with the region of the percolation threshold when sharp changes take place in the structure of microemulsions.

We studied in detail the reaction kinetics at various temperatures above and below the percolation threshold. The kinetic dependences of the observed rate constant on the surfactant concentration at 15–25 °C, *i.e.*, at temperatures below the clusterization threshold of the micelles, are presented in Fig. 4. In the AOT–*n*-nonane–water system, the process is retarded by almost an order of magnitude compared to the reaction in water. As the surfactant and water concentrations increase, the observed rate constant decreases. This trend is typical for the case where the reaction occurs in the surface layer^{16–18} and is due to dilution of the reactants on the increase in the volume of the aqueous phase and the interface surface. Analysis of the kinetic data at different temperatures (see Fig. 4) made it possible to calculate the activation energy and the pre-exponential factor, which are presented in Table 2. For any composition of the micellar system, the Arrhenius equation holds, as indicated by linearity of the $\log k_{obs} - 1/T$ plot with the correlation coefficient $R \geq 0.9$. The E_a values depend only slightly on the AOT concentration and water and fall in the 29.0–34.5 kJ mol^{−1} range; the $\log A$ values also change insignificantly (3.1–4.0) upon variation of the composi-

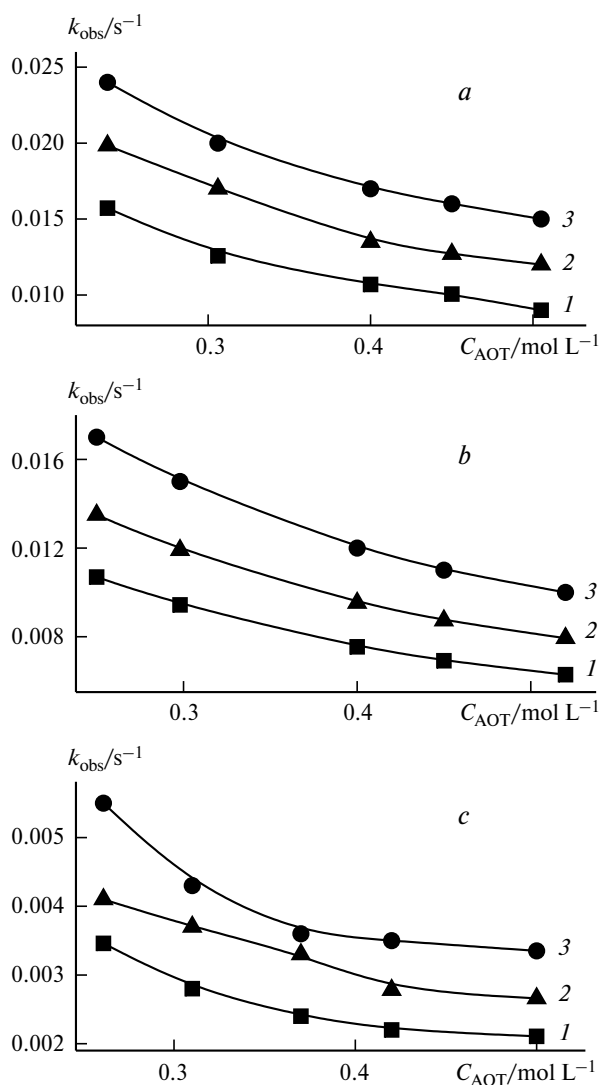


Fig. 4. Observed rate constant of the alkaline hydrolysis of phosphonate **1** (k_{obs}) vs. surfactant concentration in the AOT–*n*-nonane–water reverse micellar system at $W = 9.8$ (a), 15.1 (b), and 20.0 (c) and $T = 15$ (1), 20 (2), and 25 °C (3) ($C_{NaOH} = 0.01$ mol L^{−1}).

tion. The Arrhenius parameters for an aqueous solution in the absence of a surfactant ($E_a = 33.7$ kJ mol^{−1}, $\log A = 4.0$) fall in these ranges. These results provide the conclusion that the reaction mechanism does not change when the reaction is transferred from an aqueous solution to the micellar pseudo-phase and on rather broad variation of the micellar composition. The calculated activation energies for the alkaline hydrolysis below the percolation threshold given in Table 2 are in good agreement with the values given in Table 1, which confirms the assumption concerning the predominant contribution of the activation of chemical reaction to the temperature dependence of the rate constant below the percolation threshold.

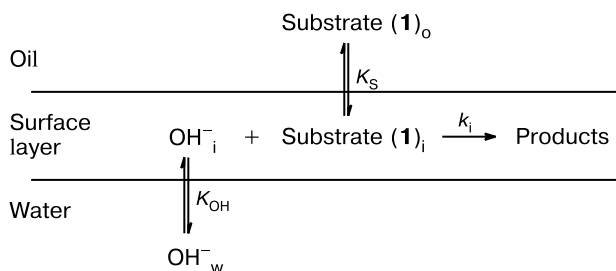
As noted above, Eq. (1) implies distribution of the substrate between the oil phase and the surface layer and

Table 2. Arrhenius equation parameters (activation energy (E_a /kJ mol⁻¹) and pre-exponential factor (log A)) for alkaline hydrolysis of phosphonate **1** in the AOT–*n*-nonane–water reverse micellar system

C_{AOT} /mol L ⁻¹	$W = 9.8$		$W = 15.1$		$W = 20.0$	
	E_a	log A	E_a	log A	E_a	log A
0.24	30.3	3.7	31.0	3.7	33.0	3.5
0.31	30.3	3.7	33.3	4.0	30.6	3.0
0.40	33.5	4.1	33.0	3.9	29.0	3.1
0.45	33.5	4.1	33.3	3.9	33.1	3.4
0.50	34.5	4.0	32.9	3.8	33.3	3.4

Note. In water without a surfactant $E_a = 33.7$ kJ mol⁻¹, log $A = 4.0$.

distribution of the nucleophile (hydroxide ion) between the aqueous core and the surface layer (Scheme 3). It is necessary that the partition constants be independent of the microemulsion composition. The graphical analysis of the kinetic data at various temperatures below the percolation threshold is shown in Fig. 5. The substrate binding constants found by graphical solution of Eq. (2) are presented in Table 3.

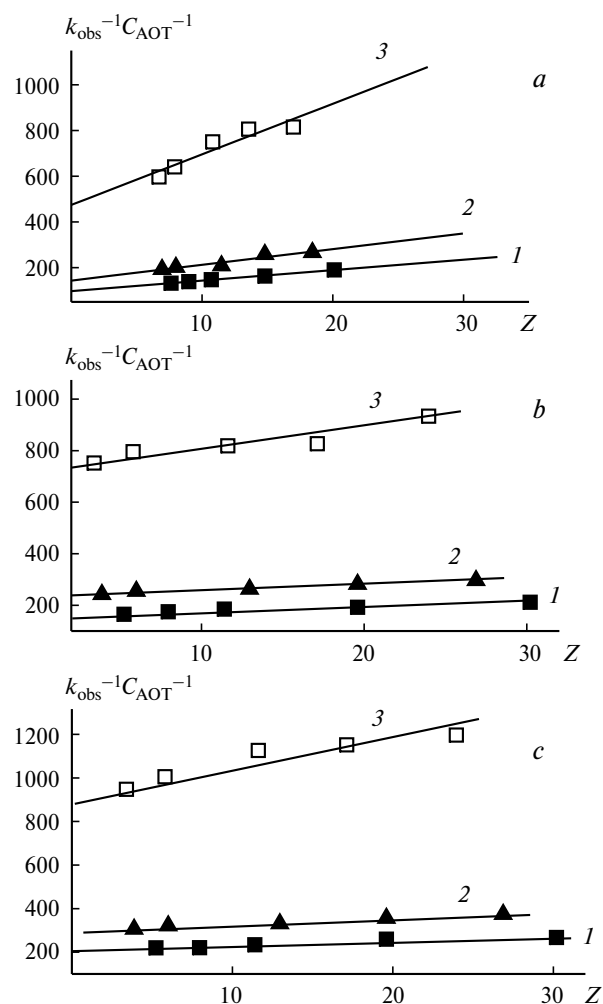
Scheme 3

It was found that Eqs (1) and (2) hold for all temperatures, as indicated by the linearity of the $1/k_{\text{obs}}C_{\text{AOT}}-Z$ plot (see Fig. 5) and by similarity of the K_S values obtained upon variation of W (see Table 3). This means that below the percolation threshold, the reaction proceeds only in the surface layer. Typically, the K_S values at 15

Table 3. Results of quantitative analysis of the kinetic data at different temperatures using graphical solution of Eq. (2)

W	$T = 15\text{ }^{\circ}\text{C}$			$T = 20\text{ }^{\circ}\text{C}$			$T = 25\text{ }^{\circ}\text{C}$		
	a	b	K_S	a	b	K_S	a	b	K_S
9.8	188.3	4.2	45.0	143.1	3.4	42.1	97.2	4.5	21.3
15.1	269.9	5.7	47.6	214.4	4.5	47.6	143.4	6.9	20.8
20.0	530.1	19.2	43.7	656.3	15.1	43.5	474.4	22.1	21.4

Note. a is the y -intercept; b is the slope of the intercept

**Fig. 5.** Linearization of the kinetic data presented in Fig. 4 using Eq. (2) for $T = 15$ (a), 20 (b), and $25\text{ }^{\circ}\text{C}$ (c) and $W = 9.8$ (1), 15.1 (2), and 20.0 (3).

and $20\text{ }^{\circ}\text{C}$ are almost equal, being both 45 ± 3 (see Table 3), i.e., $>50\%$ of the substrate is located in the surface layer at any composition of the micellar system. This is in good agreement with NMR data for self-diffusion. At $25\text{ }^{\circ}\text{C}$, the binding constant of the substrate is twice lower, which is apparently due to reactant redistribution taking place as the temperature approaches the percolation threshold. The other parameters of Eq. (1) at $25\text{ }^{\circ}\text{C}$ are as follows: $K_{\text{OH}} = 1.9$, $k_i = 3.9\text{ s}^{-1}$. The $k_{2,1}$ value was calculated from the relation $k_{2,1} = k_i V$. Assuming that $V = 0.37\text{ L mol}^{-1}$,¹¹ one gets $k_{2,1} = 1.44\text{ L mol}^{-1}\text{ s}^{-1}$. The results of calculations allow one to draw conclusions on what factors determine the effect of microemulsions on the reactivity of phosphonates. According to known data,¹⁹ changes in the microenvironment properties (micellar microenvironment factor) and in the local reactant concentration (concentrating factor) upon transfer of the reaction factors from a molecular solution to micelles are the main factors respon-

sible for the catalytic action of micellar systems. One component of the microenvironment factor can be compared with the solvent effect: this includes the medium polarity, the efficiency of solvation of the reactants and the transition state, *etc.* This contribution can be conventionally designated as the enthalpy constituent of the microenvironment factor. In addition, the transfer of the reaction to the micellar pseudophase may also change the entropy contribution, which takes into account the degree of mobility and the mutual orientation of the reactants (configuration of the activated complex). The microenvironment factor can be described quantitatively by the $k_{2,i}/k_{2,w}$ value ($k_{2,w} = 4.0 \text{ L mol}^{-1} \text{ s}^{-1}$), which is equal to 0.36. From this, it follows that the inhibitory effect of the AOT–*n*-nonane–water system in the hydrolysis of phosphonate **1** is mainly due to the adverse influence of the reactant microenvironment in the surface layer. The factor of reactant concentrating, which plays the crucial role in normal micelles, does not exert a significant effect in reverse micellar systems. This is apparently due to the low partition constant of hydroxide ions.

The dependences of k_{obs} on the medium composition at 40 °C, *i.e.*, above the percolation threshold, are presented in Fig. 6. When comparing the data presented in Figs 4 and 6, one can note several essential differences. First, above the percolation threshold, k_{obs} shows the opposite dependence on W , in particular, the rate constant

increases with an increase in the water content, while the tendency of the rate constant to decrease with an increase in the surfactant concentration is retained. Second, for $W = 9.8$ and 15.1 above the percolation threshold, k_{obs} substantially decreases (by up to an order of magnitude) as the temperature rises from 25 to 40 °C. For $W = 20.0$ and high AOT concentrations, the k_{obs} values at 25 and 40 °C are almost equal, while for $[\text{AOT}] < 0.38 \text{ mol L}^{-1}$, the rate constant at 40 °C is somewhat higher than that at 25 °C. At 40 °C, the variations of k_{obs} upon the variation of the system composition are more pronounced than at low temperatures (*cf.* Fig. 4). For instance, an increase in the surfactant concentration at an invariable water content induces a 3 to 4-fold decrease in k_{obs} , while the variation of W at a constant surfactant concentration results in a 7-fold change in the rate constant. Below the percolation threshold, variation of the surfactant concentration changes k_{obs} at most 1.5-fold, and upon the variation of W , the k_{obs} value changes 5-fold.

Unlike the plots presented in Fig. 4, the kinetic data for 40 °C cannot be linearized in the coordinates of Eq. (2), as indicated by the scatter of points and the negative slope of the plots (Fig. 7). Apparently, due to the system perturbation near and above the clusterization temperature, the distribution of the reactants is not described by Scheme 3 and the reaction zone is not confined to the surface layer. According to the data presented in Fig. 1, the temperature-induced variations of the microemulsion state are substantially different depending on its composition, *i.e.*, at the same temperature, the reactants may occur under different conditions depending on the surfactant concentration and water content, and the application of Eq. (1) becomes illegitimate. The fact that Eq. (1) does not hold above the percolation threshold is convincing evidence confirming the change in the distribution and location of the reactants and, hence, in the nature of their microenvironment.

Study of the absorption spectra of *p*-nitrophenol, a product of the reaction under consideration used to monitor the reaction kinetics, has shown (Fig. 8) that raising the temperature in the 25–40 °C range entails a decrease in the intensity of the absorption band at $\lambda = 400 \text{ nm}$, *i.e.*, the proportion of the dissociated form of the compound decreases. This fact indicates that the acid properties of *p*-nitrophenol decrease on temperature rise. The decrease in the absorbance (see Fig. 8) is much more pronounced than the expected change caused by the temperature dependence of the extinction coefficient, which is observed for an aqueous solution of *p*-nitrophenol or in the AOT–*n*-nonane–water reverse system beyond the percolation transition area. The presence of a substantial polarity gradient in reverse micelles (dielectric permeability changes from 2–4 in the bulk pseudophase to 80 in the aqueous core at a high degree of hydration) provides the conclusion that the observed shift of the compound

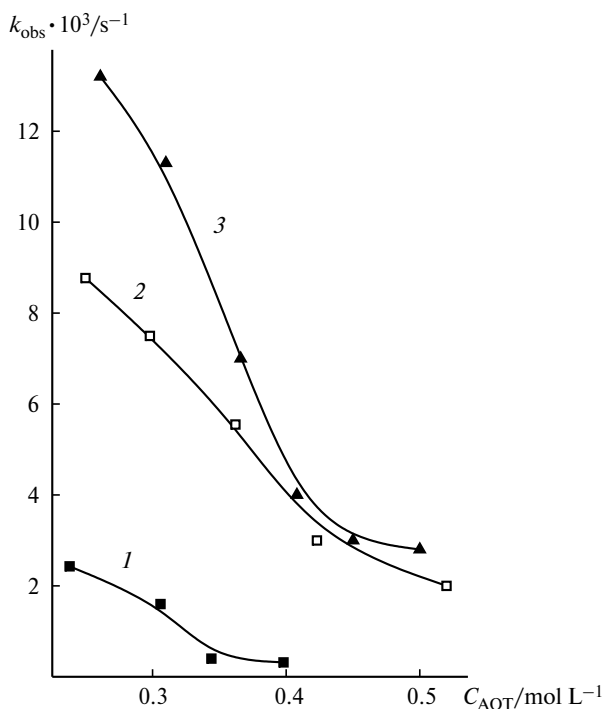


Fig. 6. Observed rate constant of the alkaline hydrolysis of phosphonate **1** (k_{obs}) vs. surfactant concentration (C_{AOT}) in the AOT–*n*-nonane–water reverse micellar system at $W = 9.8$ (1), 15.1 (2), and 20.0 (3) ($T = 40 \text{ °C}$; $C_{\text{NaOH}} = 0.01 \text{ mol L}^{-1}$).

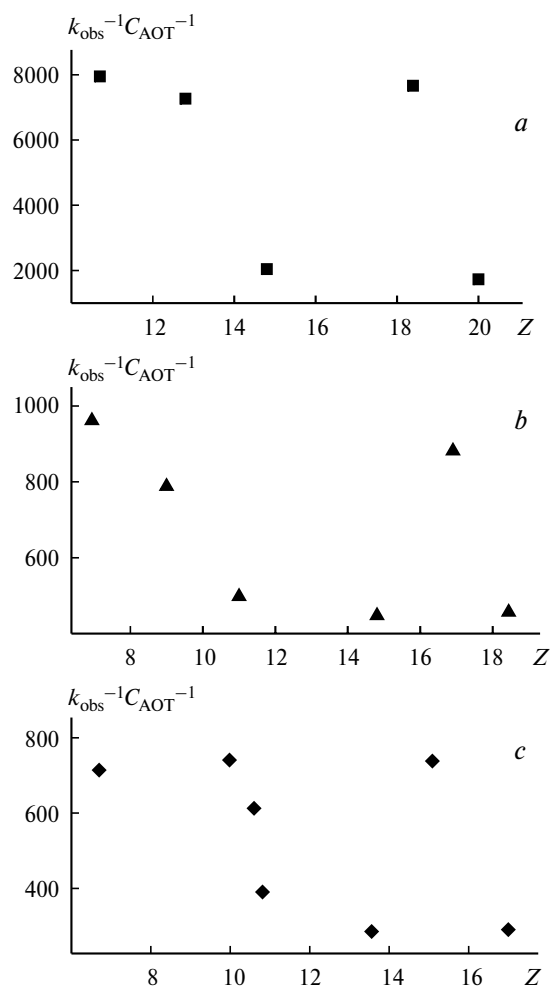


Fig. 7. Linearization of the kinetic data presented in Fig. 6 using Eq. (2): $W = 9.8$ (a), 15.1 (b), and 20.0 (c).

pK_a is caused by the change in its location site following temperature rise and by the transfer of the reaction to a zone with a reduced micropolarity.

Thus, the reactivity of phosphonate **1** in the AOT—*n*-nonane—water system changes in the vicinity of the temperature percolation threshold. The reason is the change in the reactant location sites and, hence, in the microscopic properties of the solution in the solubilization region as a result of clusterization of microemulsion drops. Studies of the reactant location sites by NMR self-diffusion and optical spectroscopy and modeling of the kinetics within the framework of the pseudophase approach indicate that below the percolation threshold, the reaction occurs in the surface layer. Under these conditions, the reactivity of compounds in microemulsions, like that in an aqueous solution, is described by the Arrhenius equation; the activation energy and $\log A$ change slightly on the transfer of the reaction from the aqueous pseudophase to the micellar phase and on variation of the

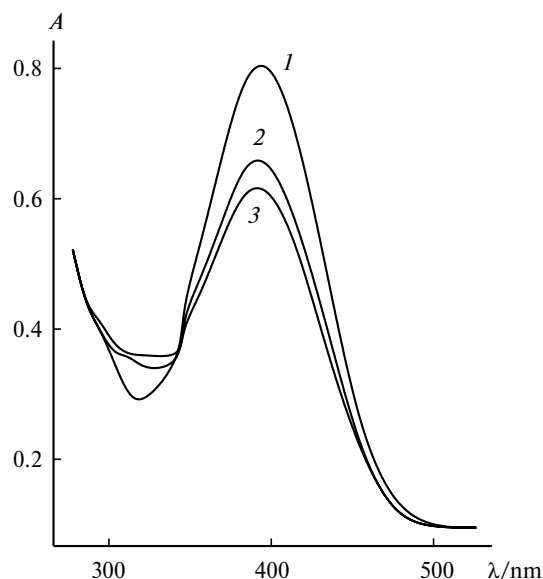


Fig. 8. Absorption spectra of *p*-nitrophenol in the visible region at 25 (1), 30 (2), and 40 °C (3) ($C_{\text{AOT}} = 0.4 \text{ mol L}^{-1}$, $C_{\text{NaOH}} = 0.01 \text{ mol L}^{-1}$).

solution composition. Above the percolation threshold, the reaction zone is not confined to the surface layer. In this case, the reactivity of phosphonate **1** does not obey the Arrhenius equation, the pattern of temperature dependence of the observed rate constant for hydrolysis substrate **1** being determined by the change in the local properties of the reactant microenvironment on temperature rise.

This study was financially supported by the Russian Foundation for Basic Research (Project No. 05-03-08086).

References

1. *Microemulsions: Structure and Dynamics*, Eds S. E. Friberg and P. Bothorel, CRC Press, Boca Raton, 1987.
2. Yu. L. Khmel'nitskii, A. V. Levashov, N. L. Klyachko, and K. Martinek, *Usp. Khim.*, 1984, **53**, 545 [*Russ. Chem. Rev.*, 1984, **53** (Engl. Transl.)].
3. Y. Feldman, N. Kozlovich, I. Nir, and N. Garti, *Phys. Rev. E*, 1995, **51**, 478.
4. C. Cametti, P. Codastefano, P. Tartaglia, S.-H. Chen, and J. Rouch, *J. Phys. Rev. A*, 1992, **45**, 5358.
5. Yu. Feldman, N. Kozlovich, I. Nir, N. Garti, V. Archipov, Z. Idiyatullin, Yu. Zuev, and V. Fedotov, *J. Phys. Chem.*, 1996, **100**, 3745.
6. J. Lang, N. Lalem, and R. Zana, *J. Phys. Chem.*, 1992, **96**, 4667.
7. L. Ya. Zakharova, F. G. Valeeva, L. A. Kudryavtseva, N. L. Zakhartchenko, and Yu. F. Zuev, *Mendeleev Commun.*, 1998, 224.

8. V. E. Bel'skii, L. A. Kudryavtseva, O. M. Il'ina, and B. E. Ivanov, *Zhurn. Obshch. Khim.*, 1970, **49**, 2470 [*J. Gen. Chem. USSR*, 1970, **49** (Engl. Transl.)].
9. S. Perez-Casas, R. Castillo, and M. Costas, *J. Phys. Chem. B*, 1997, **101**, 7043.
10. P. Stilbs, *Prog. NMR Spectrosc.*, 1987, **19**, 1.
11. L. Garcia-Rio, J. R. Leis, J. C. Mejuto, M. E. Pena, and E. Iglesias, *Langmuir*, 1994, **10**, 1676.
12. P. Stilbs, *J. Colloid Interface Sci.*, 1982, **87**, 385.
13. O. Söderman and P. Stilbs, *Progr. NMR Spectrosc.*, 1994, **26**, 445.
14. P.-G. Nilsson and B. Lindman, *J. Phys. Chem.*, 1983, **87**, 4756.
15. R. Schmidt and V. N. Sapunov, *Non-Formal Kinetics*, Verlag Chemie, Weinheim, 1982.
16. L. Garcia-Rio, P. Herves, J. C. Mejuto, J. Perez-Juste, and P. Rodriguez-Dafonte, *Ind. Eng. Chem. Res.*, 2003, **42**, 5450.
17. L. Ya. Zakharova, F. G. Valeeva, R. A. Shagidullina, L. A. Kudryavtseva, *Izv. Akad. Nauk. Ser. Khim.*, 2000, 1366 [*Russ. Chem. Bull., Int. Ed.*, 2000, **49**, 1360].
18. A. R. Ibragimova, F. G. Valeeva, L. Ya. Zakharova, L. A. Kudryavtseva, N. M. Azancheev, S. N. Shtykov, L. S. Shtykova, and I. V. Bogomolova, *Zhurn. Fiz. Khim.*, 2004, **78**, 1186 [*Russ. J. Phys. Chem.*, 2004, **78** (Engl. Transl.)].
19. I. V. Berezin, K. Martinek, and A. K. Yatsimirskii, *Usp. Khim.*, 1973, **42**, 1729 [*Russ. Chem. Rev.*, 1973, **42** (Engl. Transl.)].

Received July 22, 2004;
in revised form November 26, 2004